Mon. Not. R. Astron. Soc. **336,** 309–314 (2002)

A very massive spectroscopic binary in the LH 54 OB association in the Large Magellanic Cloud

Pablo G. Ostrov★

Facultad de Ciencias Astronómicas y Geofísicas, Paseo del Bosque S/N (1900) La Plata, Argentina

Accepted 2002 June 6. Received 2002 May 18; in original form 2002 May 1

ABSTRACT

We announce the discovery of a new early-type, double-lined spectroscopic binary in the LH 54 OB association in the Large Magellanic Cloud. We present a *V* light curve and radial velocities. We investigate the possible configurations of the system, concluding that it probably contains the most massive star measured at the present, with a mass of the order of 100 $M_\odot$, while its companion has approximately 50 $M_\odot$.

Key words: binaries: eclipsing – stars: early-type – stars: fundamental parameters – stars: individual: LH 54-425 – Magellanic Clouds.

1 INTRODUCTION

Though we can trust that the present development of stellar-interior modelling qualitatively reproduces the consecutive stages along the evolution of stars, there still remain appreciable quantitative discrepancies between theoretical predictions and empirical evidence, especially in that concern to the higher mass stars. That is not surprising because, on one hand, their modelling is intrinsically more difficult due to their more complex evolution, and on the other hand, very massive stars are rare because of its shorter lifetimes, so that there are scarce observational constraints.

During the last years, we have performed a campaign of observations of early Magellanic stars in order to enrich the empirical knowledge of these objects, particularly in low-metallicity regions.

One of the new binaries discovered, the light curve of which was completed, is a $V \sim 13$ mag star in the LH 54 OB association (Lucke & Hodge 1970). This star ($\alpha = 5^{\rm h}26^{\rm m}24^{\rm s}$, $\delta = -67^\circ 30' 13''$) is bright enough and has sufficiently large radial velocity excursions to be at scope of the 2.15-m telescope at CASLEO[1] (San Juan, Argentina) for radial velocity measurements.

Hill, Madore & Freedman (1994) identified this object as LH 54-425 and performed *UBV* photometry, obtaining $V = 13.19 \pm 0.01$, $B - V = -0.31 \pm 0.01$ and $U - B = -1.02 \pm 0.01$. Later on, Oey (1996a) obtained $V = 13.13 \pm 0.007$, $B - V = -0.215 \pm 0.014$ and $U - B = -1.010 \pm 0.015$, listing this star as L54S-4. CCD spectra were also obtained by Oey (1996b) with the ARGUS multifiber spectrograph at the CTIO 4-m telescope. The spectral type assigned by Oey to this star was O4 III (f*). She did not detect double lines at the phase of her observation.

LH 54-425 is the earliest star of the OB association LH 54, located at the east side of the superbubble DEM 192 (Davies, Elliot & Meaburn 1976) (or N51D, Henize 1956) that is probably related with its growth (Oey & Smedley 1998).

2 OBSERVATIONS

LH 54 had been included in one of our selected fields for searching new eclipsing binaries. It was observed during four observing runs between 1998 and 2001.

LH 54-425 showed no eclipses, but exhibited small periodic luminosity changes of the order of ∼0.1 mag, suggesting an ellipsoidal nature of the variability. For this reason we included it as subject for further spectroscopic study as soon as its light curve was sufficiently complete to compute a reasonably reliable ephemeris.

2.1 Photometry

CCD images of the region of LH 54 were obtained at CASLEO between 1998 and 2001, with the same instrumentation described in Ostrov, Lapasset & Morrell (2000). We derived a *V* light curve from aperture photometry performed with DAOPHOT (Stetson 1987, 1991), and tied all the measurements to a unique instrumental system using several stars as local standards to reduce errors, as described in Ostrov et al. (2000). We performed absolute photometry during a photometric night (1998 December 3), obtaining $V = 13.05 \pm 0.015$, and $B - V = -0.121 \pm 0.011$. Table 1 displays our photometric measurements of LH 54-425, corrected to the standard system, together with the internal errors derived from the local standards, the full width at half maximum (FWHM) and the airmass for each frame.

2.2 Spectroscopy

Spectroscopic observations were obtained by means of a REOSC spectrograph in its single dispersion mode, attached to the 2.15-m

★E-mail: ostrov@fcaglp.edu.ar

[1]Complejo Astronómico El Leoncito, operated under agreement between the Consejo Nacional de Investigaciones Científicas y Técnicas de la República Argentina and the National Universities of La Plata, Córdoba and San Juan.

Table 1. *V* light photometry of LH 54-425.

HJD 245 0000+	V	σ_i	FWHM (arcsec)	X	HJD 245 0000+	V	σ_i	FWHM (arcsec)	X
1149.807	13.087	0.011	2.09	1.30	1503.601	13.048	0.008	2.62	1.48
1149.834	13.061	0.011	2.36	1.36	1503.687	13.058	0.006	2.86	1.27
1150.847	13.082	0.012	1.91	1.40	1503.742	13.059	0.007	2.40	1.23
1151.617	13.067	0.006	1.92	1.33	1503.795	13.069	0.005	2.84	1.25
1151.671	13.059	0.008	2.04	1.25	1503.836	13.069	0.004	2.83	1.30
1151.731	13.050	0.004	2.00	1.23	1504.575	13.048	0.006	3.46	1.58
1151.786	13.056	0.006	2.13	1.28	1504.628	13.046	0.007	3.14	1.39
1151.857	13.048	0.006	2.05	1.44	1504.736	13.050	0.008	3.49	1.23
1152.663	13.085	0.005	2.26	1.26	1504.776	13.051	0.007	2.72	1.24
1152.709	13.076	0.007	1.98	1.23	1504.814	13.053	0.006	3.00	1.27
1152.751	13.073	0.005	2.19	1.24	1504.842	13.060	0.007	3.16	1.32
1152.800	13.066	0.006	1.98	1.31	1859.592	13.058	0.007	3.62	1.63
1152.831	13.062	0.006	1.86	1.37	1859.615	13.059	0.005	3.18	1.53
1153.692	13.105	0.007	1.62	1.23	1859.652	13.052	0.006	3.04	1.40
1153.735	13.106	0.006	1.76	1.24	1859.683	13.052	0.004	3.51	1.32
1153.768	13.092	0.006	1.87	1.26	1859.709	13.054	0.005	4.02	1.28
1153.823	13.079	0.005	2.36	1.36	1859.721	13.045	0.019	6.23	1.26
1153.857	13.070	0.008	2.40	1.46	1859.763	13.063	0.013	6.23	1.23
1154.706	13.110	0.005	2.06	1.23	1859.806	13.046	0.004	5.11	1.24
1154.740	13.100	0.005	2.16	1.24	1859.838	13.047	0.007	4.63	1.26
1154.804	13.102	0.007	2.48	1.32	1860.592	13.092	0.010	5.08	1.62
1154.845	13.096	0.004	2.45	1.43	1860.687	13.073	0.006	5.37	1.31
1155.674	13.105	0.005	2.03	1.24	1860.760	13.065	0.005	3.87	1.23
1155.712	13.111	0.004	1.99	1.23	1860.832	13.070	0.006	5.22	1.26
1155.748	13.115	0.005	2.05	1.25	1860.867	13.053	0.005	4.74	1.31
1155.776	13.116	0.005	1.86	1.28	1861.604	13.109	0.007	3.65	1.55
1155.826	13.115	0.007	2.49	1.38	1861.733	13.092	0.005	4.05	1.25
1155.851	13.108	0.006	2.56	1.45	1861.815	13.075	0.004	3.37	1.25
1499.825	13.090	0.004	2.90	1.27	1861.860	13.067	0.006	3.66	1.31
1500.589	13.089	0.011	3.61	1.56	1862.572	13.112	0.007	3.65	1.69
1500.659	13.101	0.004	2.89	1.34	1862.638	13.109	0.006	3.44	1.42
1500.732	13.107	0.004	3.01	1.24	1862.698	13.109	0.006	3.26	1.28
1500.799	13.110	0.007	3.19	1.24	1862.751	13.099	0.005	3.36	1.23
1500.844	13.104	0.006	3.34	1.30	1862.833	13.092	0.005	3.53	1.27
1501.549	13.068	0.005	3.30	1.76	1863.564	13.104	0.005	2.64	1.72
1501.593	13.077	0.007	3.38	1.53	1863.634	13.117	0.007	3.08	1.42
1501.616	13.079	0.007	3.25	1.45	1863.720	13.118	0.004	2.69	1.25
1501.677	13.090	0.004	3.10	1.30	1863.810	13.116	0.004	3.45	1.25
1501.756	13.098	0.005	2.60	1.23	1864.619	13.084	0.006	2.27	1.46
1501.815	13.106	0.004	3.00	1.26	1864.681	13.093	0.006	1.79	1.30
1502.565	13.047	0.008	3.93	1.65	1864.755	13.108	0.005	2.38	1.23
1502.699	13.078	0.009	2.36	1.26	1864.812	13.119	0.006	2.80	1.25
1502.784	13.083	0.008	2.12	1.24	2212.865	13.071	0.006	2.82	1.26
1502.832	13.089	0.008	2.14	1.29	2213.797	13.060	0.005	2.74	1.23
1502.861	13.096	0.018	3.99	1.34	2214.855	13.062	0.006	1.99	1.25

telescope at CASLEO. The CCD detector was the same Tektronik used for photometry. We used a 600 mm^{-1} grating giving a reciprocal dispersion of 1.63 Å $pixel^{-1}$ on the range from 3900 to 5500 Å. Our resolution, measured from the Cu–Ne–Ar comparison lamp lines, was 2 pixels.

We obtained spectra near the quadratures in series of three 1200 s exposures. The spectrograms were processed and extracted using IRAF routines. Each series of three observations was combined in one spectrogram, before performing the concomitant measurements.

3 ANALYSIS

3.1 Ephemeris

We applied two period search methods to the photometric data: one derived from Lafler & Kinman (1965) and the one described in Shwarzenberg-Czerny (1997). Because of our short time-base and the intrinsically small light variations, we can not derive a precise ephemeris. We found that the most probable period is $P = 2.2475$ d, with aliases each 0.007 d. We used

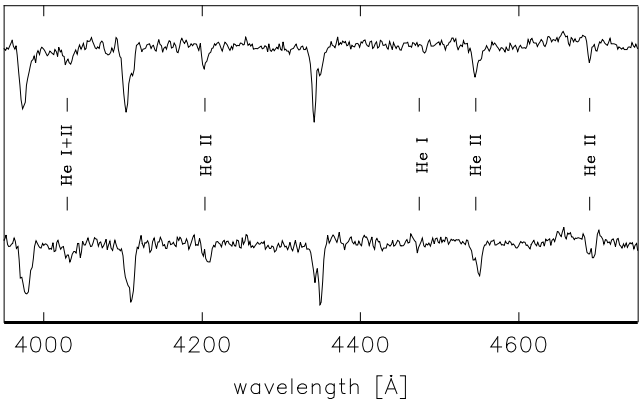

Figure 1. CCD spectra of LH 54-425 obtained at CASLEO, corresponding to both quadratures.

this period and $E_0 = 245\,2216.597$ to plan the spectroscopic observations.

3.2 Spectroscopic classification

We classified the spectra following the criteria of Walborn & Fitzpatrick (1990). The earliest component shows no lines of He I, corresponding thus an O3 spectral type. The other component shows He I 4471 hardly visible due our poor signal-to-noise ratio (in fact, it is only detectable in our best spectrograms, obtained during dark nights) and more intense He II lines, which is in agreement with an approximately O5 type. With regard to the luminosity classes, we combined all the spectrograms acquired in each quadrature to increment the signal to noise ratio. In the averaged spectrograms, N IV 4058 emission from the primary is visible, together with Si IV λλ 4089 or 4116 depending on the phase (this is alternatively blended with the Hδ absorption of the secondary). We are not able to assign a luminosity class to the secondary. Therefore, we classify the system as O3 III (f*) + O5. Fig. 1 shows the CCD spectrograms of LH 54-425 obtained during dark nights, corresponding to both quadratures.

3.3 Radial velocity measurements

The He II 4686-Å line appears clearly double in all our spectrograms. He II 4200 and He II 4542 appear double in some spectrograms and severely blended in others. The He II absorption pairs were measured by means of a double Gaussian fit using the 'deblend' function of the 'SPLOT' IRAF task. Only the easily separable He II pairs were used for the radial velocity determinations. Table 2 lists the heliocentric radial velocities derived for both binary components, together with that corresponding to the nebular [O III]λ5007 emission, used to check the stability of the system.

Table 2. Radial velocities.

HJD−245 0000	Phase	Primary (km s^{-1})	Secondary (km s^{-1})	[O III] (km s^{-1})
2286.732	0.702	122	679	286
2287.721	0.146	500	19	286
2329.516	0.742	114	704	269
2330.537	0.197	496	−169	280
2330.645	0.245	450	−119	280
2331.546	0.646	96	648	284

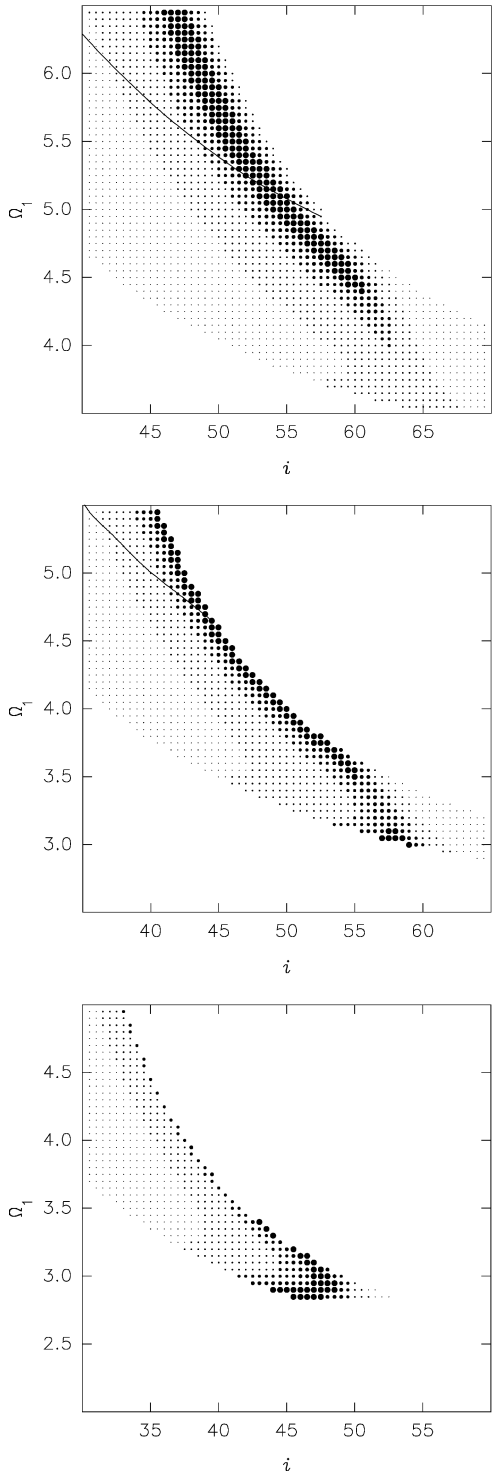

Figure 2. Residuals of the detached models. Points of different sizes represent the sums of squared residuals, the bigger symbols corresponding to the smaller amounts. The limits between different point sizes are 1.65, 3.30, 4.95 and 8.24 times the sum of squared residuals of the best-fitting model. The different panels correspond to different assumed effective temperatures and total luminosity of the system, as quoted in the text.

3.4 Exploration of the geometry of the system

Because the system shows no true eclipses, it is not possible to derive reliable physical parameters just from the light curve and radial velocities. For this reason, we assumed an absolute magnitude

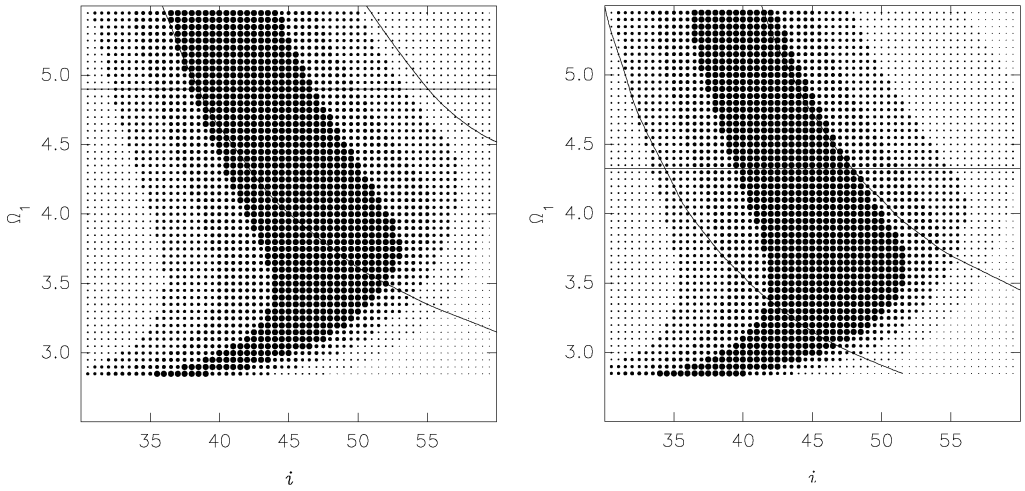

Figure 3. Residuals of the semi-detached models. Points of different sizes represent the sums of squared residuals, as in Fig. 2. The left- and right-hand panels correspond to different assumed temperature scales, as quoted in the text.

and investigated which system configurations were compatible with the observations.

We computed the models with the Wilson–Devinney codes (Wilson 1990; Wilson & Devinney 1971). For the bolometric albedos and gravity darkening coefficients we assumed values of $A = 1.0$ and $g = 1.0$, respectively, which are adequate for radiative envelopes (Rucinski 1969; Lucy 1976). For the limb darkening a square root law (Díaz-Cordovés & Giménez 1992) was used, taking the corresponding coefficients from tables by Díaz-Cordovés, Claret & Giménez (1995).

3.4.1 Detached configurations

We first explored the possible detached configurations, so the mode of operation 2 of the Wilson–Devinney program was chosen. In order to reduce the degrees of freedom of the problem, we fixed the total bolometric magnitude of the system. We considered three cases, with $M_{\rm bol} = -10$, -10.3 and -10.6. For the models with $M_{\rm bol} = -10$ we assigned temperatures of 52 500 K and 44 500 K, corresponding to spectral types O3 V and O5 V according to Schmidt-Kaler (1982), while for those models with $M_{\rm bol} = -10.6$ we adopted the temperature scale of Chlebowski & Garmany (1991) for O3 III and O5 III stars, 46 500 K and 42 300, respectively. For the models with intermediate bolometric magnitude we used the mean of the two temperature scales. With this procedure, the extreme cases in distance moduli and temperature scales were considered.

For each adopted orbital inclination, temperature and potential Ω_1 of the primary, the secondary's potential Ω_2 was chosen according to the assumed total bolometric magnitude of the system.

Fig. 2 displays the results of the experiments with detached configurations. Points of bigger size represent smaller O–C light curve residuals. The lower limit corresponds to the primary being 2.5 mag brighter than the secondary component, which can be rejected according to the relative intensity of the corresponding spectral lines. The upper limit corresponds to semi-detached configurations, with the secondary star filling its Roche-lobe. Models above the solid curve have the secondary brighter than the primary, therefore they also can be disregarded.

The upper panel, which corresponds to highest temperatures and lower luminosity, shows that the best-fitting models are near the semi-detached configuration, with the secondary filling its Roche lobe. These models are not realistic from an evolutionary perspective, as they have secondary components of bigger size than the primary components. If the less massive star is the more evolved one, we have to conclude that mass inversion has occurred, and the system is now semi-detached.

In the middle panel we considered models with intermediate luminosities and temperatures. The best solutions are aligned at the upper limit of the models considered, indicating a semi-detached configuration. There are also good models with $\sim 58^\circ$ and $\Omega_1 \sim 3$. It means that the *primary* star is almost filling its Roche lobe. However, it is not very plausible, because the magnitude difference between both stars is nearly 2.5 mag, which does not agree with the spectroscopic evidence.[2]

The residuals from models with lowest temperature scale and highest total luminosity (which allows the biggest sizes of the stars) are presented in the bottom panel. In this case, besides of the semi-detached configurations, there exist plausible detached solutions, with $i \sim 47^\circ$. The lowest value considered for the potential Ω_1 (2.85) implies that the primary component is almost filling its Roche lobe, although (as mentioned above) in these models the luminosity difference between both stars is excessive.

3.4.2 Semi-detached configurations

Considering that some results of the experiments suggested that the system is semi-detached, with the cooler and less massive star filling its Roche lobe, we explored these configurations, using therefore the mode of operation 5 in the Wilson–Devinney programs. Fig. 3 shows the residuals of these models, corresponding to the high and low temperature scales, respectively, mentioned above. As the margins of plausible models are wide, it is necessary to consider limits to the total luminosity to restrict the amount of solutions. The upper and bottom curves drawn on Fig. 3 correspond to models with $M_{\rm bol} = -10$ and $M_{\rm bol} = -10.6$, respectively, while models above the

[2]It does not allow one to disregard such solutions completely. For example, Niemelä & Bassino (1994) called 'primary' at the Roche-lobe filling component of HV 2543, based on the intensity of their spectral lines, while from the Wilson–Devinney modelling that star is approximately 0.9 *V* magnitudes fainter than its companion.

Table 3. Best-fitting plausible models.

	Adopted Values	
T_1		46 500 K
T_2		42 300 K
$M_{\rm bol}$		−10.6
	Fitted Values	
V_γ		295.0 ± 3 km s^{-1}
$q(M_2/M_1)$		0.48 ± 0.01
Configuration	Detached	Semi-detached
i (adopted)	47°	45.5°
Ω_1 (adopted)	3.1	3.15
Ω_2	2.86[a]	2.84[b]
a	38.1 ± 0.4 R$_\odot$	39.3 ± 0.4 R$_\odot$
Σres^2	0.0033222	0.0033563
	Star Dimensions	
M_1	100 ± 3 M$_\odot$	108 ± 3 M$_\odot$
R_1	15.1	15.1 R$_\odot$
$M_{\rm bol1}$	−10.2	−10.2
log g_1[cgs]	4.1 ± 0.1	4.1 ± 0.1
M_2	48.4 ± 3 M$_\odot$	52.2 ± 3 M$_\odot$
R_2	11.9 R$_\odot$	12.4 R$_\odot$
$M_{\rm bol2}$	−9.3	−9.3
log g_2 [cgs]	4.0 ± 0.1	4.0 ± 0.1

[a]Chosen according the total luminosity of the system.
[b]$\Omega_{\rm crit}$.

horizontal line have the secondary more luminous than the primary component. Configurations with Ω_1 smaller than those plotted in the graphics are in 'overcontact', and can be also rejected according to the assumed limits in the total luminosity of the system.

4 RESULTS

In spite of the wide range of models that can fit the observations well, we can state with reasonable confidence that the inclination is roughly $45^\circ \sim 50^\circ$, since bigger values would cause eclipses. This implies that the masses are ∼100 and ∼50 M$_\odot$ for the O3 and the O5 component, respectively. Table 3 summarizes the parameters that best fit suitable detached and semi-detached solutions. It must be noted that the errors quoted in Table 3 correspond to fixed values of i, Ω_1 and Ω_2, i.e. the errors of the masses reflect only the errors in the radial velocity measurements.

The modelled light and radial velocity curves are displayed in Figs 4 and 5, together with the observations and O–C residuals. The models correspond to the best-fitting detached configuration, although there are not visible difference with the best-fitting semi-detached solution.

In the more modest case, the inclination is $i \sim 58^\circ$ and the corresponding masses are ∼64 and ∼31 M$_\odot$, although this model have a primary 2.3-mag brighter than the secondary component, which is not supported by the spectroscopic data. (The other extreme case, where both stars are of similar brightness, corresponds to $i \sim 39^\circ$ and gives masses of ∼160 and ∼80 M$_\odot$.) All possible solutions indicate that this system contains the more massive star measured at the present.

In a previous work (Ostrov 2001) we found from the analysis of another early Magellanic binary with O3 I f* and O6 V components, and masses of 41 and 27 M$_\odot$. That was an overcontact system, with a still shorter period of only 1.4 d. These results suggests that extremely early stars have a wide range of masses, at least when they belong to very close binaries, where mass exchange and mass loss play a fundamental role in the evolution.

Indeed, observations of these systems with higher signal to noise and dispersion than that reachable at CASLEO would provide valuable data to investigate the similitudes and differences between these objects.

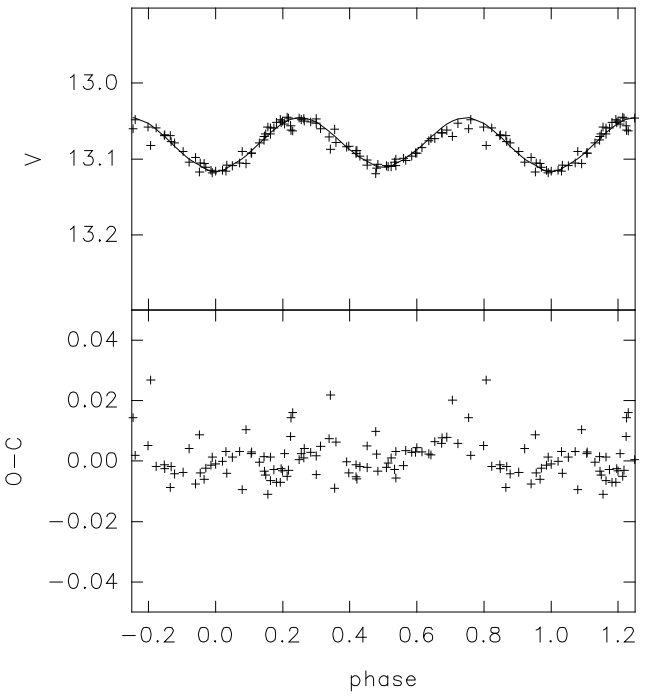

Figure 4. The observed and modelled *V* light curve for LH 54-425 and their concomitant O–C residuals.

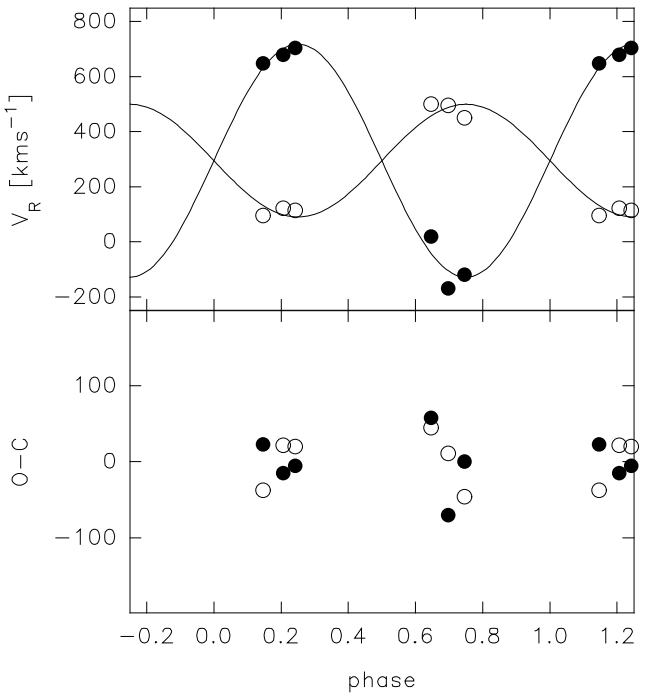

Figure 5. Observed and modelled radial velocity curve for LH 54-425 and their O–C residuals. Hollow circles correspond to the primary component and filled ones stand for the secondary.

ACKNOWLEDGMENTS

I wish especially to thank Dr Claudia Giordano for help with English, and Dr Nidia Morrell for helpful comments. The author acknowledge use at CASLEO of the CCD and data acquisition system supported through US National Science Foundation grant AST-90-15827 to R. M. Rich. The focal reducer in use at CASLEO was kindly provided by Dr M. Shara. The IRAF software is distributed by NOAO, operated by AURA for the NSF. This research has made use of the Astronomical Data Centre catalogues. I would also like to thank the referee, Dr Otmar Stahl, for suggestions that allowed me to clarify some issues in the paper.

REFERENCES

Chlebowski T., Garmany D., 1991, ApJ, 368, 241
Davies R. D., Elliot K. H., Meaburn J., 1976, Mem. R. Astron. Soc., 81, 89
Díaz-Cordovés J., Giménez A., 1992, A&A, 259, 227
Díaz-Cordovés J., Claret A., Giménez A., 1995, A&AS, 110, 329
Henize K. G., 1956, ApJS, 2, 315
Hill R. J., Madore B. F., Freedman W. L., 1994, ApJS, 91, 538
Lafler J., Kinman T. D., 1965, ApJS, 11, 216
Lucke P. B., Hodge P. W., 1970, AJ, 75, 171
Lucy L. B., 1976, ApJ, 205, 208
Niemelä V. S., Bassino L. P., 1994, ApJ, 437, 332
Oey M. S., 1996a, ApJS, 104, 71
Oey M. S., 1996b, ApJ, 465, 231
Oey M. S., Smedley S. A., 1998, AJ, 116, 1263
Ostrov P. G., 2001, MNRAS, 321, L25
Ostrov P. G., Lapasset E., Morrell N. I., 2000, A&A, 356, 935
Rucinski S. M., 1969, Acta Astron., 19, 245
Schmidt-Kaler Th., 1982, in Shaifers K., Voigt H. H., eds, Landolt-Börnstein, New Ser., Group VI, Vol. 2/b. Springer Verlag, Berlin–Heidelberg
Shwarzenberg-Czerny A., 1997, ApJ, 489, 941
Stetson P. B., 1987, PASP, 99, 191
Stetson P. B., 1991, in Grosbøl P. J., Warmel R. H., eds, 3rd ESO/ST-ECF Data Analysis Workshop. ESO, Garching, p. 187
Walborn N. R., Fitzpatrick E. L., 1990, PASP, 102, 650
Wilson R. E., 1990, ApJ, 356, 613
Wilson R. E., Devinney E. J., 1971, ApJ, 166, 605

This paper has been typeset from a TEX/LATEX file prepared by the author.